

# Robustness of the P-U and lnD-U loop wave speed estimation methods: Effects of the diastolic pressure decay and vessel wall non-linearities

Jonathan P. Mynard, Malcolm R. Davidson, Daniel J. Penny, and Joseph J. Smolich

**Abstract**—Arterial wave speed estimated invasively from pressure ( $P$ ) and velocity ( $U$ ) measurements using the P-U loop method, or non-invasively from diameter ( $D$ ) and  $U$  measurements using the lnD-U loop method, assume that during early systole 1) backward-running waves are absent and 2) wave speed is constant. These assumptions also form the basis of a method for correcting time lags between  $P$  (or lnD) and  $U$  in which the  $R^2$  of the early-systolic linear regression is maximized. However, neither of the two assumptions are strictly valid *in vivo*, where the diastolic pressure decay from the previous beat may give rise to some non-zero backward-running  $P$ ,  $U$  and wave intensity ( $WI$ ) components, and the pressure-dependency of wave speed may lead to curvilinearity in the early-systolic P-U and lnD-U relations. Accordingly, this study assessed the robustness of three phase correction algorithms, (including two that are not dependent on the two assumptions stated above, i.e., aligning the times of the peak 2nd derivative or peak signal curvature) and of the P-U and lnD-U loop wave speed estimation methods under a range of diastolic decay rates and degrees of vessel wall non-linearity. Results from a simple computer model of the arterial circulation suggested that although an apparent phase lag may be introduced by assuming linearity, the magnitude of this phase lag is likely to be small considering the sample intervals normally used in experimental studies; however, under highly non-linear flow conditions, the apparent lag may be comparable to hardware-related lags. Predicted errors in estimated wave speed using the P-U loop method were generally less than 10%, while somewhat higher errors were found in the lnD-U loop method (up to 15-20%). In both, higher diastolic pressure decay rates were associated with higher wave speed errors, although this effect was eliminated by subtracting the extrapolated diastolic pressure curve from the measured pressure. Overall, each of the time lag correction algorithms and wave speed estimation methods were generally satisfactory, although further experimental work is required to assess the curvature-based phase correction method and pressure adjustment *in vivo*.

## I. INTRODUCTION

Accurate estimation of wave speed from experimental data is crucial for gaining information about vessel properties and for the analysis of pressure ( $P$ ), velocity ( $U$ ) and wave intensity ( $WI$ ) [1]–[3]. The most commonly-employed technique for estimating wave speed in invasive studies is the P-U loop method [1], while a similar method proposed recently for non-invasive studies is the lnD-U loop method that employs measurements of diameter ( $D$ ) and  $U$  [2].

J.P. Mynard was supported by a Dora Lush Biomedical Scholarship from the National Health and Medical Research Council of Australia.

J.P. Mynard, D.J. Penny and J.J. Smolich are with the Heart Research Group, Murdoch Childrens Research Institute and the Department of Paediatrics, University of Melbourne, Parkville, VIC, Australia jonathan.mynard@mcri.edu.au

M.R. Davidson is with the Department of Chemical and Biomolecular Engineering, University of Melbourne, Parkville, VIC, Australia

Before applying these methods, hardware-related time lags between  $U$  and  $P$  or  $D$  need to be corrected [1], [4], which in previous studies has been achieved by shifting the velocity signal to align the peak second derivatives of  $P$  and  $U$  [3], [5] or to achieve the most linear relationship (i.e. highest  $R^2$ ) between  $P$  (or  $D$ ) and  $U$  during early systole [1], [6].

However, the wave speed estimation methods and the phase correction algorithm based on maximizing  $R^2$  assume that 1) backward-running waves are minimally present during early systole and 2) wave speed is constant throughout the cardiac cycle, neither of which are strictly valid *in vivo*. Regarding the first assumption, the diastolic decline of arterial pressure is not completed by the start of the next beat, suggesting that backward-running waves may not be completely absent during early systole [7]. Moreover, since wave speed is actually pressure-dependent and varies during the cardiac cycle [8], the early-systolic P-U or lnD-U relations may, in fact, be curvilinear and not linear.

Although early-systolic backward waves and the pressure-dependency of wave speed are generally considered to exert negligible effects, it is unclear to what extent these phenomena introduce error into the P-U or lnD-U loop wave speed estimation methods, or produce apparent time lags between  $P$  (or  $D$ ) and  $U$ . This study investigates these issues using a simple computer model of the arterial circulation in which wave speed is known *a priori* and no phase lag is present. Three time lag correction algorithms are assessed, 1) the maximal  $R^2$  regression method [1], [6], 2) the peak second-derivative alignment method [3], [5] and 3) a new method proposed here in which the onset of  $P$  and  $U$  signals, as assessed by peak curvature [9], [10], are aligned; note that unlike the first of these three methods, the last two do not depend on an assumption of linearity. The accuracy of the obtained time lags and P-U or lnD-U loop-estimated wave speeds are assessed under a wide range of diastolic decay rates and flow conditions that range from linear to highly non-linear.

## II. METHODS

The model of the systemic arterial circulation consists of a single one-dimensional (1D) segment, representing the wave propagation phenomena in the large arteries, and a 3-element windkessel (0D) compartment representing the peripheral vasculature (Figure 1). The equations governing instantaneous pressure ( $P$ ), velocity ( $U$ ) and cross-sectional area ( $A$ ) are given by

$$\frac{\partial A}{\partial t} + \frac{\partial AU}{\partial x} = 0 \quad (1)$$

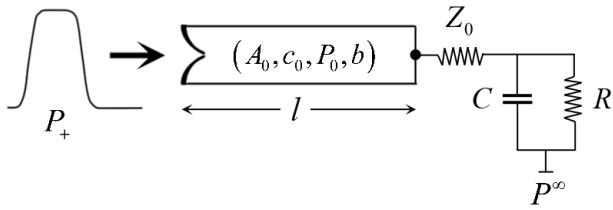


Fig. 1. Schematic of the single segment computer model, where unless otherwise stated,  $l = 7$  cm,  $A_0 = 6$  cm<sup>2</sup>,  $c_0 = 4$  m/s,  $P_0 = 80$  mmHg,  $b = 2.8$ ,  $Z_0 = \rho c_0 / A_0 = 0.053$  mmHg.s/mL,  $C = 1.0$  mL/mmHg,  $R = 1.0$  mL/mmHg,  $P^\infty = 35$  mmHg. Parameters chosen to produce normal aortic pressure, velocity and wave intensity signals [1], [5].

$$\frac{\partial U}{\partial t} + U \frac{\partial U}{\partial x} + \frac{1}{\rho} \frac{\partial P}{\partial x} = -22\pi\mu \frac{U}{A} \quad (2)$$

where  $\mu$  is blood viscosity and  $\rho$  is blood density (0.035 poise and 1.06 g/cm<sup>3</sup> respectively). A non-linear pressure-area relation (or ‘wall law’) is given by

$$P - P_{\text{ext}} = \frac{2\rho c_0^2}{b} \left[ \left( \frac{A}{A_0} \right)^{b/2} - 1 \right] + P_0 \quad (3)$$

where  $P_{\text{ext}}$  is external pressure (assumed to be zero) and the reference cross-sectional area ( $A_0$ ), wave speed ( $c_0$ ) and pressure ( $P_0$ ) are assumed to be uniform along the entire length ( $l$ ) of the 1D segment. The wall law power ( $b$ ) governs the non-linearity of the pressure-area relation and thus the degree to which wave speed depends on pressure, as seen via the following expression for instantaneous wave speed,

$$c = \sqrt{\frac{b}{2\rho} (P - P_0) + c_0^2} \quad (4)$$

At the inlet to the 1D segment, a ‘forward pressure’ ventricle/valve model is employed and has been described previously along with the numerical techniques used for solving the 1D governing equations and for coupling 1D and 0D domains [11], [12]. The 3-element windkessel consists of a characteristic impedance ( $Z_0$ ), compliance ( $C$ ), peripheral resistance ( $R$ ) and outlet pressure ( $P^\infty$ ). Note that the time constant ( $\tau$ ) of the diastolic pressure decay is approximately equal to  $R(C + C_{1D})$ , where  $C_{1D} = A_0 l / (\rho c_0^2)$  is the compliance of the 1D segment, and is thus varied by changing  $C$ . Parameter values are given in the caption of Figure 1.

The theory of wave intensity analysis has been described elsewhere [13], [14]. Briefly, time-corrected  $WI$  is defined as  $(dP/dt)(dU/dt)$  and may be separated into forward and backward-running components,  $WI_\pm = (dP_\pm/dt)(dU_\pm/dt)$ , where the pressure and velocity components are given by

$$P_\pm = \frac{1}{2} (P \pm \rho c U) + P_\pm^0 \quad (5)$$

$$U_\pm = \frac{1}{2} \left( U \pm \frac{1}{\rho c} P \right) + U_\pm^0 \quad (6)$$

where, for graphing purposes, the arbitrary initial values are assumed to be  $P_\pm^0 = P_{\text{ed}}$  and  $U_\pm^0 = 0$ , with  $P_{\text{ed}}$  being end-diastolic pressure. Since linear wave separation is

performed, the cycle-averaged wave speed ( $\bar{c}$ ) is used and is considered the true wave speed against which P-U or lnD-U loop estimates are compared.

If wave travel is unidirectional, the water hammer equation ( $dP_\pm = \rho c dU_\pm$ ) leads to the following expression for wave speed ( $c_{PU}$ ) using single-site measurements of  $P$  and  $U$ ,

$$c_{PU} = \frac{1}{\rho} \frac{dP_\pm}{dU_\pm} \quad (7)$$

Thus if  $c$  is constant, the relationship between arterial  $P$  and  $U$  during early systole is expected to be linear, with a slope equal to  $\rho c$  [1]. Similarly, the relation between vessel distensibility ( $D_s$ ) and wave speed ( $c^2 = 1/(\rho D_s)$ ) can be used to estimate wave speed ( $c_{DU}$ ) from single-site measurements of  $D$  and  $U$  as follows [2],

$$c_{DU} = \pm \frac{1}{2} \frac{dU_\pm}{d \ln D_\pm} \quad (8)$$

Again, the relation between  $\ln(D)$  and  $U$  is expected to be linear during early systole, with a slope of  $1/(2c)$ . Note however, that a pressure-dependence of wave speed is likely to cause some degree of curvilinearity in the early-systolic  $P-U$  and  $\ln D-U$  relations, even in the absence of any backward-running waves or time lags. To eliminate the effect of the diastolic pressure decay on early-systolic backward waves, the diastolic pressure is fitted to a mono-exponential curve, extrapolated into the next beat and subtracted from the raw pressure to yield an adjusted pressure.

The new method for correcting time lags is motivated from previous work [9], [10], which demonstrated that peaks in signal curvature provide an accurate means of identifying the early-systolic onset or ‘foot’ of a haemodynamic signal. The curvature ( $\kappa$ ) of a continuous signal ( $y$ ) is defined as

$$\kappa(t) = \frac{d^2 y / dt^2}{\left[ 1 + (dy/dt)^2 \right]^{3/2}} \quad (9)$$

A discrete version of this function for use with time signals, derived in [10], is given by

$$k(t_i) = \frac{\frac{2}{\Delta x^2} \sum_{m=-2}^2 a_2^m y_{i+m}}{\left[ 1 + \left( \frac{1}{\Delta x} \sum_{m=-2}^2 a_1^m y_{i+m} \right)^2 \right]^{3/2}} \quad (10)$$

where  $a_k^m$  refers to the  $m$ th coefficient and  $k$ th derivative obtained from a fourth-order Savitzky-Golay filter.  $\Delta x$  is a constant that transforms the time axis into an axis that is approximately orthogonal to the  $y$  axis; for full details see [10].

### III. RESULTS & DISCUSSION

Fig. 2 shows the simulated net  $P$  and  $U$  signals (black lines) and the forward (red) and backward (blue) components of  $P$ ,  $U$  and  $WI$ . In Fig. 2A, it can be seen that the diastolic decay in the previous beat persists into the next beat and causes a small change in  $P_-$  and  $U_-$  and a non-zero value of  $WI_-$  during early systole (as indicated by the arrows). Moreover, when wave speed is highly pressure-dependent

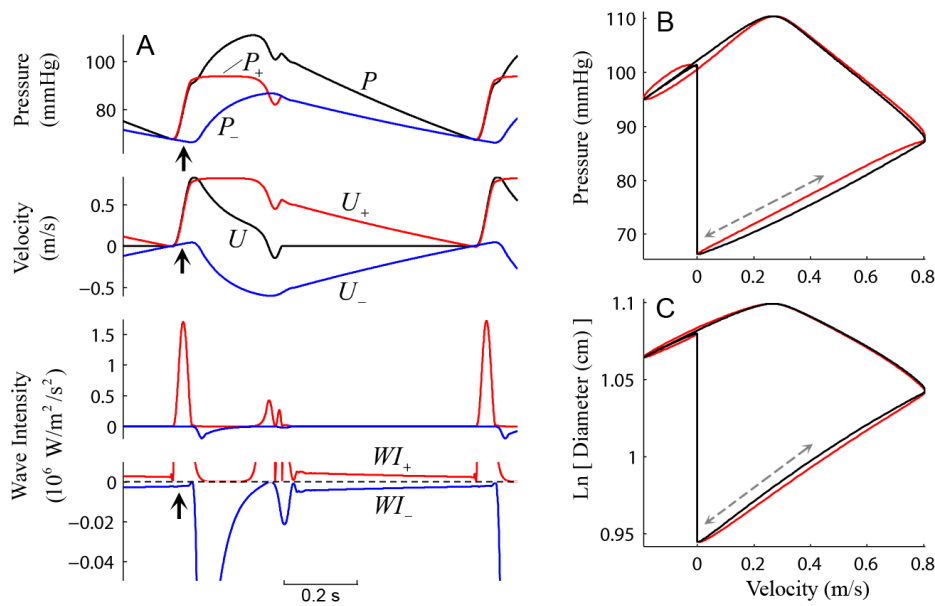


Fig. 2. (A) Model-derived net pressure and velocity ( $P$  and  $U$ , black lines) and the forward (red) and backward (blue) components of pressure ( $P_{\pm}$ ), velocity ( $U_{\pm}$ ) and wave intensity ( $WI_{\pm}$ ) for linear flow conditions ( $b = 0.1$ ). The arrows show that  $P_-$  and  $U_-$  are changing during early systole, while  $WI_-$  is non-zero. (B) The  $P$ - $U$  loop and (C) the  $\ln D$ - $U$  loop under non-linear flow conditions ( $b = 8.5$ ). The black loops are from the model and display some curvilinearity during early-systole (indicated by the grey dashed arrows). The red loops result from the velocity time lag correction algorithm in which the lag is determined by the maximal  $R^2$  of the early-systolic regression.

(ranging from 2.9 at end-diastole to 5.7 at peak pressure,  $b = 8.5$ ), the early-systolic part of the  $P$ - $U$  (Fig. 2B) and  $\ln D$ - $U$  (Fig. 2C) loops display some curvilinearity (black loops), whereas shifting the velocity signal in order to maximize the  $R^2$  of the respective relationships during this time (red loops) suggests the existence of a time lag between the raw signals when none is present.

The magnitude of the apparent shift is shown in Fig. 3 for the three different phase correction algorithms and over a range of arterial time constants (A) and degrees of vessel wall non-linearity (B). Comparison of the correction algorithms before (solid lines/filled symbols) and after (dashed lines/open symbols) adjustment of the pressure to remove the effect of the diastolic decay in the previous beat indicates that although such adjustment alters the apparent time lag, it has no clear benefit. Note that previous high-fidelity wave intensity studies have used sampling rates of up to 1000 Hz [3], [5] and therefore a shift of 1 ms represents at most only one sample interval. The predicted apparent shifts in Fig. 3A&B are thus generally quite small. However, with increasingly non-linear conditions (higher  $b$ ), the apparent phase lag progressively increases for all of the correction algorithms except the curvature-based method, approaching the same magnitude as the hardware-related lags reported for transit-time flow probes (3.5 ms) [15].

The corresponding errors in estimated wave speed using the  $P$ - $U$  loop method are given in Fig. 3C&D, while the errors for the  $\ln D$ - $U$  loop method are shown in Fig. 3E&F. In most cases, the  $P$ - $U$  and  $\ln D$ - $U$  loop methods underestimate and overestimate wave speed respectively. When the raw pressure is used in the calculations (solid lines), the error magnitude increases (up to 12%) with smaller time

constants (i.e. higher decay rates, Fig. 3C&E), whereas with the adjusted pressure, the errors are smaller and no longer dependent on the time constant. These findings support the notion that a faster diastolic decay rate degrades the accuracy of wave speed estimation techniques, although the resultant errors are generally less than 10% even for fast decay rates. With the  $P$ - $U$  loop method, increasing the degree of non-linearity (Fig. 3D) causes progressive changes to the wave speed errors except when the curvature-based phase correction algorithm is used. Use of the adjusted pressure leads to absolute errors that are mainly less than 5%, although the raw pressure used in conjunction with the maximal  $R^2$  lag correction algorithm also results in accurate estimates of wave speed (despite inaccurate estimates of the phase lag, Fig. 3B). Using the raw pressure, the  $\ln D$ - $U$  loop method exhibits greater errors compared with the  $P$ - $U$  loop method, which increase progressively to between 15 and 20% at high degrees of non-linearity (Fig. 3E). These errors are only partially ameliorated by the pressure adjustment, while results derived in conjunction with the curvature-based lag correction algorithm lead to appreciably lower errors. Overall, comparison of panels D and F in Fig. 3 suggest that non-linearities have a greater confounding influence on the  $\ln D$ - $U$  loop method compared with the  $P$ - $U$  loop method.

#### IV. CONCLUSIONS

Modelling results presented in this study indicate that a pressure-dependence of wave speed may lead to apparent shifts between  $P$  (or  $\ln D$ ) and  $U$  and that both vessel wall non-linearity and rapid diastolic decay rates (or low arterial time constants) may introduce error into arterial wave speed estimates obtained from the  $P$ - $U$  or  $\ln D$ - $U$  loop methods.

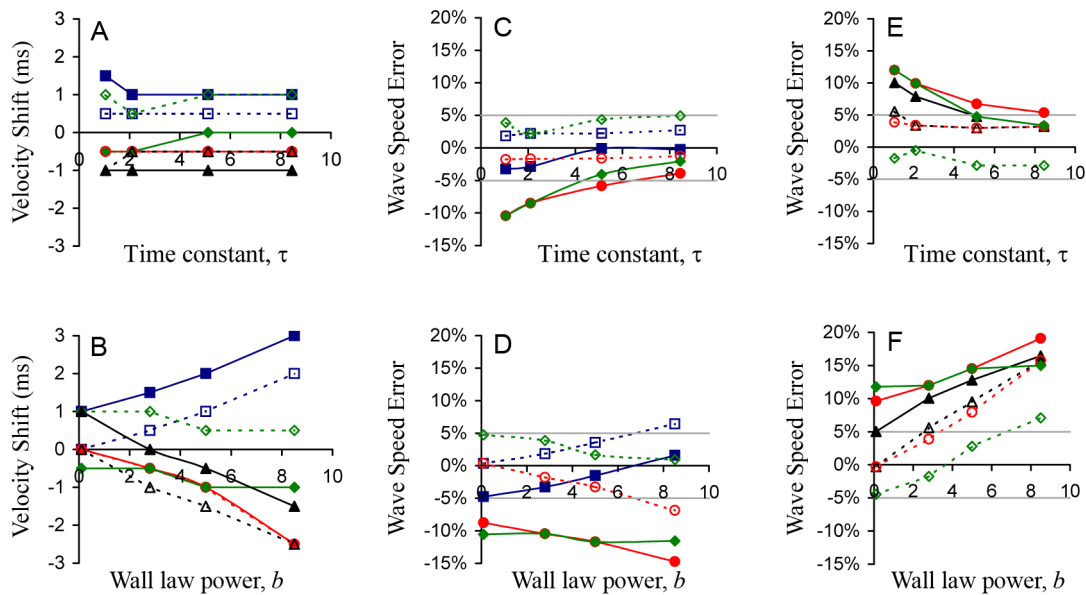


Fig. 3. The velocity shift introduced by the time lag correction algorithms when (A) the arterial time constant ( $\tau$ ) is varied, resulting in a wide range of diastolic decay rates, and (B) the wall law power ( $b$ ) is varied (higher values mean a greater pressure-dependence of wave speed). The algorithms tested are the maximal  $R^2$  method using the P-U loop (blue squares) or lnD-U loop (black triangles), the 2nd-derivative alignment method (red circles) and the peak curvature alignment method (green diamonds). These algorithms were applied using the raw pressure signal (solid lines/filled symbols) or the adjusted pressure (i.e. after subtracting the extrapolated diastolic decay from the previous beat, dashed lines/open symbols). (C,D) The corresponding errors in estimated wave speed when assessed via the P-U loop method (symbols as in panels A & B). (E,F) The errors in estimated wave speed when assessed via the lnD-U loop method (symbols as in panels A&B). 5% error lines are shown with grey lines in panels C-F.

Although the maximal  $R^2$  and peak 2nd derivative alignment methods appear to be reliable under most circumstances, they may become less accurate under highly non-linear flow conditions. By contrast, a new phase correction method proposed here, in which the peaks in signal curvature are aligned, appears to be insensitive to the degree of non-linearity. Although wave speed estimates obtained from the P-U and lnD-U loop methods appear to be accurate to within  $\sim 10\%$  under most circumstances, their accuracy may be improved (particularly for lower arterial time constants) by a pressure adjustment in which the extrapolated diastolic pressure decay from the previous beat is subtracted from the measured signal. Further work is required to evaluate the curvature-based phase correction method and pressure adjustment procedure *in vivo*.

#### REFERENCES

- [1] A. W. Khir, A. O'Brien, J. S. Gibbs, and K. H. Parker, "Determination of wave speed and wave separation in the arteries," *J Biomech*, vol. 34, no. 9, pp. 1145–55, 2001.
- [2] J. Feng and A. W. Khir, "Determination of wave speed and wave separation in the arteries using diameter and velocity," *J Biomech*, vol. 43, no. 3, pp. 455–462, 2010.
- [3] J. J. Smolich, J. P. Mynard, and D. J. Penny, "Ductus arteriosus wave intensity analysis in fetal lambs: Midsystolic ductal flow augmentation is due to antegrade pulmonary arterial wave transmission," *Am J Physiol Regul Integr Comp Physiol*, vol. 297, no. 4, pp. R1171–1179, 2009.
- [4] J. P. Mynard, J. J. Smolich, and D. J. Penny, "Wave intensity analysis (WIA): Flow velocity lags influence calculated ascending aortic wave speed and reflected wave intensity during beta-adrenergic stimulation," *J Mol Cell Cardiol*, vol. 41, no. 4, p. 742, 2006.
- [5] D. J. Penny, J. P. Mynard, and J. J. Smolich, "Aortic wave intensity analysis of ventricular-vascular interaction during incremental dobutamine infusion in adult sheep," *Am J Physiol Heart Circ Physiol*, vol. 294, no. 1, pp. H481–489, 2008.
- [6] M. J. P. Swalen and A. W. Khir, "Resolving the time lag between pressure and flow for the determination of local wave speed in elastic tubes and arteries," *J Biomech*, vol. 42, no. 10, pp. 1574–1577, 2009.
- [7] J. Alastruey, "On the mechanics underlying the reservoir-excess separation in systemic arteries and their implications for pulse wave analysis," *Cardiovasc Eng*, vol. 10, no. 4, pp. 176–89, 2010.
- [8] M. B. Hisland and M. A. X. Anliker, "Influence of flow and pressure on wave propagation in the canine aorta," *Circ Res*, vol. 32, no. 4, pp. 524–529, 1973.
- [9] J. P. Mynard, D. J. Penny, and J. J. Smolich, "A semi-automatic feature detection algorithm for hemodynamic signals using curvature-based feature extraction," in *29th Ann Int Conf IEEE Eng Med Biol Soc*, 2007, pp. 1691–1694.
- [10] —, "Accurate automatic detection of end-diastole from left ventricular pressure using peak curvature," *IEEE Trans Biomed Eng*, vol. 55, no. 11, pp. 2651–2657, 2008.
- [11] J. P. Mynard and P. Nithiarasu, "A 1D arterial blood flow model incorporating ventricular pressure, aortic valve and regional coronary flow using the locally conservative Galerkin (LCG) method," *Comm Num Meth Eng*, vol. 24, no. 5, pp. 367–417, 2008.
- [12] J. P. Mynard, M. R. Davidson, D. J. Penny, and J. J. Smolich, "A numerical model of neonatal pulmonary atresia with intact ventricular septum and RV-dependent coronary flow," *Int J Num Meth Biomed Eng*, vol. 26, no. 7, pp. 843–861, 2010.
- [13] K. Parker, "An introduction to wave intensity analysis," *Med Biol Eng Comput*, vol. 47, no. 2, pp. 175–188, 2009.
- [14] J. Mynard, D. J. Penny, and J. J. Smolich, "Wave intensity amplification and attenuation in non-linear flow: Implications for the calculation of local reflection coefficients," *J Biomech*, vol. 41, no. 16, pp. 3314–3321, 2008.
- [15] E. H. Hollander, J. J. Wang, G. M. Dobson, K. H. Parker, and J. V. Tyberg, "Negative wave reflections in pulmonary arteries," *Am J Physiol Heart Circ Physiol*, vol. 281, no. 2, pp. H895–902, 2001.